

Current Density Simulations in the Electrodeposition from Ionic Liquids: Effects of the Conductivity.

I. Perissi^{*1}, C. Borri¹, S. Caporali¹, and A. Lavacchi¹

¹Department of Chemistry, University of Firenze, Via della Lastruccia, 3, 50019 – Sesto Fiorentino (FI) – Italy.

*Corresponding author: Department of Chemistry, University of Firenze, Via della Lastruccia, 3, 50019 – Sesto Fiorentino (FI) – Italy, ilaria.perissi@unifi.it

Abstract: The overall goal of this work is the use of COMSOL Multiphysics in the modelling of the current density distributions for the electrodeposition of Aluminium coatings from Ionic Liquids. The local current distribution is strongly dependant on the conductivity and on the geometry of the galvanic cell and can only be performed by the numerical solution of the PDE's governing the system. The ability to predict the local current density on an electrode is crucial to eventually evidence portions where the deposition may be invalidate.

Keywords: Current distributions, Ionic Liquids, Electrodeposition, conductivity.

1. Introduction

Recently Ionic Liquids have been applied to the deposition of coatings with a high technological potential. We demonstrated that the Aluminium electrodeposition from IL's is a suitable candidate to the substitution of the CVD (Chemical Vapour Deposition) in the field of TBC (Thermal Barrier Coatings) for the energy and aerospace industry (www.iolisurf.com). For such an application the thickness of the coatings has to fill the specification required by the turbine blades manufacturers so that the estimation of current distributions becomes indispensable. The 'a priori' calculation of the local currents is not trivial and the difficulties increase with increasing complexity of the geometry. COMSOL Multiphysics[®] permits the integration of the simulation approach with a coating deposition real experiment. In this work, several models are described, presenting aspects regarding the currents distribution on complex geometries, also illustrating the effects of the electrochemical kinetic on the solution throwing power. With the aid of modelling, we were able to design potentiostatic depositions on differently shaped objects, in particular employing the chloroaluminates IL 1-butyl-3-

methyl imidazolium heptachloroaluminate, [BMIm] Al₂Cl₇, as electrolyte, characterized by conductivity 0.75 S m⁻¹.

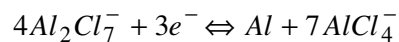
2. Governing equations.

The Laplace's Equation [1] describes current and potential distributions in conductive media, as the ILs electrolytes, in absence of charge source between the working (WE) and counter electrodes (CE) and in absence of diffusion regime.

$$\nabla^2 V = 0 \quad [1]$$

Neglecting diffusion phenomena is only valid at very low deposition rate or under strong convection which is, however, a common fact in the real experiments. Moreover, we consider that no chemical reactions occur in the bulk of the solution. Under such assumptions, two contributions concur to the total current distributions: the 'primary' current distribution, obtained neglecting the surface overpotential at the electrode interface, which describes the most non uniform approximation to an actual current distribution; the 'secondary' current distribution takes into account also the electrode polarization, which has the effect of making the current distribution more nearly uniform than the primary. To obtain a primary current distribution a constant potential boundary condition at the WE and the ground boundary condition at CE surfaces were set.

To obtain the secondary current distribution, we take into account the electrode kinetic of the Aluminium reduction, considered as 3 electrons transfer process:



A boundary condition on the potential gradient at the WE was set as the current density described by the Butler-Volmer equation [2].

The ground boundary condition at CE surfaces is imposed also in this case.

$$i = i_0 \left\{ e^{\frac{\alpha_A z F \eta}{RT}} - e^{-\frac{(1-\alpha_C) z F \eta}{RT}} \right\} \quad [2]$$

where:

i_0 = exchange current density

η = overpotential (V-E₀)

n = number of electrons

α_A = anodic charge transfer coefficient

α_C = cathodic charge transfer coefficient

The interest in a prior estimation of the primary distribution, which depends essentially by the geometry of the deposition cell, is due to the fact that it can be assumed as an index to compare with diffusive currents values: ideally, if the evaluated primary distribution remains 2-3 times lower respect the diffusive currents during all the time of deposition for every point of the WE surface, a good throwing power of the solution is realized (since the secondary distribution can only have a damping action on the primary). The 'a priori' evaluation of the primary distribution can highlight portions of the WE where currents could assume values that provoke a rapidly decrease in the reactants concentration there, and consequently, a diffusion regimes of the currents is reached.

We have conducted several experiments of galvanostatic electrodeposition on WEs of mild steel, constituted by disks with two different areas, 4.78 cm² (following named 'small disk') and 9.53 cm² (following named 'disk') respectively, and also on a turbine vane section. The registered potentials during the galvanostatic deposition (that were around 2V applying 80 A m⁻²) were employed in the simulation experiments as potential boundary conditions. Such potential ideally derives by the sum of the ohmic drop in the electrolyte and of the overpotential of the charge transfer process for the Al reduction.

The galvanic cell for the deposition on disks consists in cylindrical CE with 3.5 cm of diameter and 6.5 cm of height. The WE was put in the centre (Figure 1, a) or in a side of the cylinder (Figure 3).

Regarding the deposition on the turbine vane the galvanic cell was realized with a shaped CE as reported in figure 2.

3. Use of COMSOL Multiphysics.

In the simulation experiments we reproduced the 3D galvanostatic cell for the deposition onto the disks: due to the symmetry of the system, the estimation of the current distribution was evaluated in a portion of the cell, as represented in Figure 1, b).

A 2D representation of the deposition on the turbine vane was conducted employing the shaped counter electrode as in the 'real' experiments, and also simulations with other geometries of the CE were conducted and compared with the real experiments.

The 'Conductive media DC' model was employed to describe both the primary and secondary current distributions. The space dimension is based on 3D formulation for the

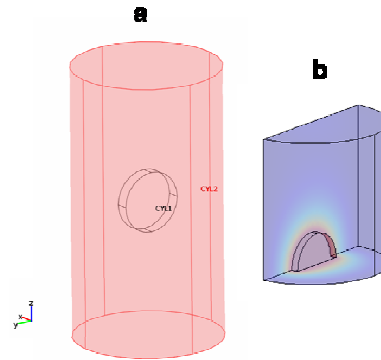


Figure 1. Geometry of the galvanic cell employed in the electrodeposition of Al from ILs on several sized disks: a, the entire geometry, b, the portion used for computation.



Figure 2. 2D Representation of the main section of the galvanic cell realized for deposition on turbine vane.

disk systems and in a 2D formulation for the turbine vane. For both the spaces, a ‘Stationary Non Linear’ with the ‘Direct UMFPACK’ solver system was used.

The solution time was dependent on the number of mesh elements. We found that meshing the CE boundary and the solution domain with a ‘coarse mesh size’ and the WE surfaces with boundary mesh parameter maximum element size $1.2 \cdot 10^{-3}$ and element grow 1.5, further refining of the meshes in both domains do not alter significantly the obtained results.

4. Results

Figure 3 shows a comparison among the geometries of cells really employed for deposition on disk shaped objects. In evidence how the size of the WE disk and its position respect to the CE influences the primary currents distributions along a cross section line profile chosen as reported in figure 3 for the respective geometry. 2V were applied as boundary condition at the WE surface. For the small disk in the centred position we obtain the highest current distribution values, with the evidence of a peak of current on the disk edge. As expected, the boundary integration of current for the applied potentials results around 3 times higher respect to the galvanostatic current density applied during electrodeposition. This is an evident proof of the presence of one or more charge transfer processes as resistances in series to the ohmic drop in the ‘real experiment’ of deposition.

For such configuration of the galvanic cell, the obtained coatings (that have been characterized elsewhere) for all the disks’ size,

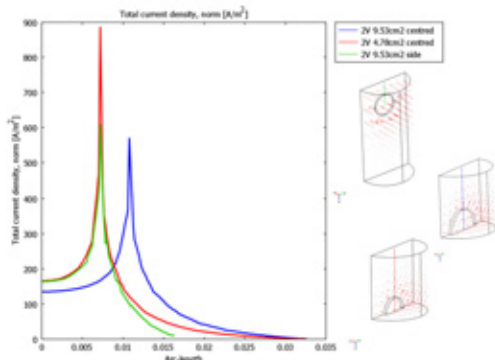


Figure 3. Primary current density profile for a cross section line of the disks: green, side small-disk; blue, centred disk; red, centred small disk.

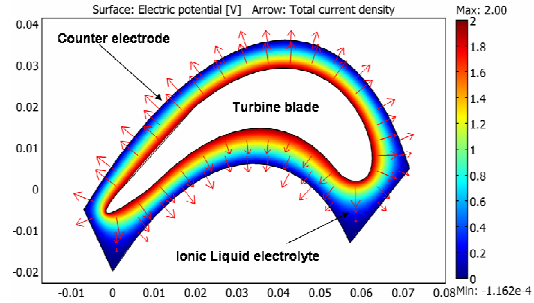


Figure 4. A 2D profiles of the current densities and of the potential distribution in the Ionic Liquids’ bath for Al electrodeposition on a turbine blade. The Aluminum counter electrode is shaped following the blade’s geometry.

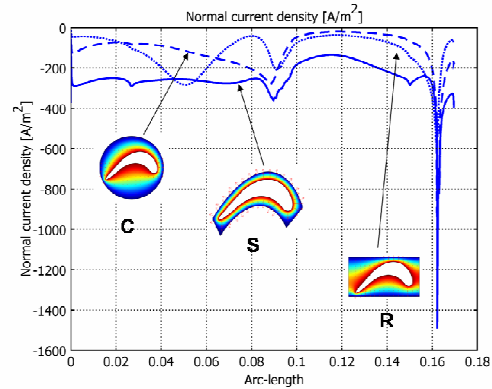


Figure 5. Primary current distributions on the turbine blade profile obtained employing different CE shapes: Circle (dashed), Shaped (solid), Rectangular (dotted). The applied potential is $E_{app}=2$ V

result in a very good quality of adhesion and uniformity with a scarce edge-effects.

More difficult has been projected a cell for deposition on the turbine vane. Figure 3 shows the real employed galvanic bath profile.

Figure 5 shows examples of the influence of the CE geometry on the primary current distribution on the turbine blade profile (WE). The best current distribution is obtained, both in term of uniformity and in term of higher current values, for the CE shaped following the turbine blade profile (S profile). The sharp peaks correspond to the blade’s tail.

For such configuration an estimation of the effect of the charge transfer process has been added to the calculation imposing the Butler Volmer equation as the boundary condition at the WE.

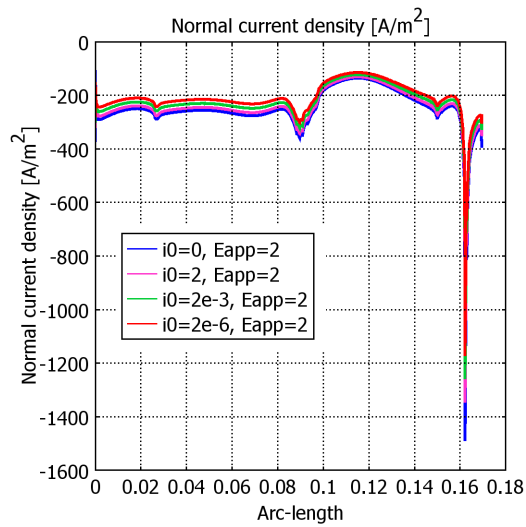


Figure 6. Primary (blue solid) and Secondary current distributions for several exchange current densities, i_0 , obtained for the S geometry. The applied potential is $E_{app}=2$ V.

Figure 6 describe the evolution of Secondary currents distribution for variations of the exchange current density, i_0 , ranging from $i_0=0$ (primary) up to $i_0=2e-6$ A m^{-2} . The damping action due to the presence of a secondary distribution for such order of conductivity becomes appreciable for phenomena with exchange current densities minor of 10^{-3} A m^{-2} .

As shows in figure 7, the turbine vane evidences two portions where the deposition had not taken place, the tail and the head at which correspond the highest values of primary current distribution.

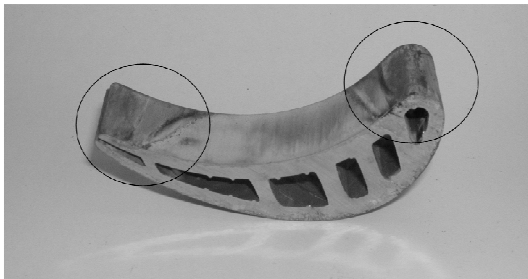


Figure 7. The circles evidence the portions of scarcely deposition of the Al on the turbine blade.

5. Conclusion

The results evidence that the current density distributions in the considered media are essentially due to the conductivity of the Ionic Liquids (around 1 S m^{-1}) and a simulation of the primary distribution is relevance to characterize critical points on the WE. For such order of conductivity, the levelling action due to the secondary currents becomes appreciable for phenomena with exchange current densities minor of 10^{-3} A m^{-2} . Thus, in the case of relatively simple electrode's shape (disks) we can successfully obtain the coatings according to the TBC specification. For more complex objects, as turbine blades, the simulations evidenced critical parts where, in the real deposition experiment, the coating does not take place.

6. References

1. A. Lavacchi , The use of FEMLAB in the electrochemical education, Paper&Presentation , <http://www.comsol.com/papers/1929/>
2. A.Lavacchi, U. Bardi, C. Borri, S.Caporali, A. Fossati, I. Perissi, Cyclic Voltammetry Simulation at Microelectrode Arrays with COMSOL Multiphysics®, *Journal of Applied Electrochemistry*, (2009).